Received: 6 February 2024 | Revised: 3 April 2024 | Accepted: 17 May 2024

DOI: 10.1002/joc.8519

RESEARCH ARTICLE

International Journal of Climatology RMetS

Climate change impacts on Central Asia: Trends, extremes and future projections

Bijan Fallah[1] | **Iulii Didovets**[1] | **Masoud Rostami**[1,2] | **Mehdi Hamidi**[3]

[1]Potsdam Institute for Climate Impact Research (PIK), Potsdam, Germany

[2]Laboratoire de Météorologie Dynamique (LMD), Sorbonne University (SU), Ecole Normale Supérieure (ENS), Paris, France

[3]Institute for Geophysics and Meteorology, University of Cologne, Cologne, Germany

Correspondence
Bijan Fallah, Potsdam Institute for Climate Impact Research (PIK), P.O. Box 601203, Potsdam 14412, Brandenburg, Germany.
Email: fallah@pik-potsdam.de

Funding information
German Federal Foreign Office; Alexander von Humboldt-Stiftung; Virgine Unite USA

Abstract

Central Asia (CA) is among the world's most vulnerable regions to climate change. Increasing anthropogenic greenhouse gas concentrations (GHGs) are the primary forcing of the current and future climate system for the time scale of a century. By analysing observation datasets, we show that a warming of 1.2°C led to a decrease of 20% in snow-depth CA during the last 70 years, especially over the mountains. In recent decades, longer summer times and fewer icing days (more than 20 days·year^{-1}) have exposed unprecedented shock to CA's climate system's components. Furthermore, we analyse 442 model simulations from Coupled Model Inter-comparison Project Phase 5 and 6 (CMIP5, CMIP6) and show that CMIP6 simulations are generally warmer and wetter than the CMIP5 ones in CA. For instance, under the highest emission scenarios (RCP8.5 and SSP5-8.5), CMIP6 projects a 6.1°C increase, while CMIP5 projects a 5.3°C increase, suggesting CMIP6 anticipates greater warming with high emissions. In contrast to CMIP6, the CMIP5 precipitation trends suggest a potential nonlinear relationship between increased greenhouse gas emissions and changes in precipitation, though the impact is much less pronounced than the temperature changes. Our analysis shows that CMIP6 models are more sensitive to temperature rise than CMIP5 ones. Both simulation sets' ensemble means capture well the observed warming trend. The imposed snow-melting leads to an increase in the run-off in the vicinity of glaciers. Such climatic shifts lead to more flooding events in CA. Given the projected warming range of 2–6°C in CA at the end of the century in various scenarios and models, such warming trends might be catastrophic in this region. The seasonal cycle of the temperature change indicates an extension of the glacier's melting period under future scenarios with fossil-fueled development. The models' uncertainty increases for the far-future time-slice, and warming larger than 4°C in CA is *very likely* among all the models and during all the seasons if no sustainable

action is taken. This study also incorporates a detailed Köppen climate classification analysis, revealing significant shifts towards warmer climate categories in Central Asia, which may have profound implications for regional hydrological cycles and water resource management, particularly in the Amu Darya and Syr Darya river basins under warmer scenario by the end of the century. The Tundra and ice cap climate categories will lose more than 60% of their coverage at the end of the century compared to the historical period in the Amu Darya and Syr Darya river basins.

KEYWORDS

Central Asia, climate change, CMIP5, CMIP6, future projections, GCM

1 | INTRODUCTION

Water availability, hydro-power and food security are the main concerns for Central Asian society in the Anthropocene era (Jalilov et al., 2016; Reyer et al., 2017). Sustainable future climate scenarios limit global warming under 2°C at the end of the century compared to pre-industrial levels (Meinshausen et al., 2020). However, the rising temperature trend in CA is already significantly above the global mean (Yao et al., 2021). Therefore, the societal and economic impacts are assumed to be severe if this threshold is crossed (Reyer et al., 2017). The climate of CA is mainly dominated by arid, semi-arid, temperate and semi-desert regions (Duan et al., 2019; Jalilov et al., 2016; Yao et al., 2021). Additionally, these regions experienced extreme nonclimatic societal and economic conditions after the collapse of the Soviet Union (Lioubimtseva & Henebry, 2009).

According to Pekel et al. (2016), more than 70% of global permanent surface water loss occurred in CA and the Middle East between 1984 and 2015. Groundwater supplies more than 36% of drinking and 42% of agricultural water globally (Ashraf et al., 2021). However, its availability is affected by increased evaporation and human withdrawals. Around 33% of Earth's population lives in semi-arid and arid regions encapsulating the Mediterranean, Asia, the Middle East and North Africa, categorized as water-stressed areas (Vörösmarty et al., 2010). A comprehensive worldwide synthesis (Vörösmarty et al., 2010) concludes that around 80% of the world's population suffers under high levels of water security.

Mountains are the most important sources of water availability for the local rivers in CA. They preserve precipitation through glaciers, permafrost and snow during winter and fall (Chen et al., 2016). Under the faster-than-global warming trend in CA, the precipitation amount and snowmelt/glacier ratio and precipitation form are modified (i.e., more rain than snow) (Chen et al., 2016). For example, more than 97% of the Tian Shan Mountains show a retreating behaviour since the 1980s (Chen et al., 2016). Kyrgyzstan is one of the countries exposed to extreme landslide hazards and extreme precipitation. Glacier melting events might contribute to landslides and floods (Saponaro et al., 2015). Generally, five countries are involved in the geopolitics of Tian Shan. Tajikistan and Kyrgyzstan are among the water providers, and Turkmenistan, Uzbekistan, and Kazakhstan are the consumers (Lemenkova, 2014). The current renewable freshwater resources in CA (cubic meters/capita) are as follows: Tajikistan (7146), Kyrgyzstan (7894), Kazakhstan (3568), Afghanistan (1299), Uzbekistan (504) and Turkmenistan (244) (data from https://data.worldbank.org). The coupled political and climate change impacts make it challenging to tackle the severe problems around water availability in CA (Duan et al., 2019). Water providers mainly use freshwater resources for hydro-power and the downstream countries for agriculture (Didovets et al., 2021).

It is well-known that global warming will accelerate the hydrological cycle based on the Clausius–Clapeyron theory (Gao et al., 2018; Robinson et al., 2021). However, how the local impacts of global warming are captured by the state-of-the-art CMIP6 climate models over CA has not been investigated. In CA, the relationship between water availability and precipitation is complicated. The glaciers and snowmelt play a vital role which could be affected by warming at different levels. The variable warming trend in CA's main glaciers, like in the Tien-shan Mountains, will accelerate the glaciers' shrinkage. The downstream countries will face water storage deficits till the end of the century (Chen et al., 2015).

The other negative impact of the warming is the extended warming season, contributing to the glaciers melting for longer periods. The warmer August and September months will be an extra stress factor to the

hydrological cycle in CA. Previous studies have explored the seasonal climate variability in the GCMs (Santer et al., 2018; Stouffer & Wetherald, 2007; van der Wiel & Bintanja, 2021). However, the spatio-temporal pattern of climate change over the CA region is less discussed.

One helpful tool for analysing compound climate change is the usage of climate classification datasets like the Köpen climate classification system, which is a widely used vegetative-based climatological framework that categorizes the world's climates based on average monthly values of temperature and precipitation (Kottek et al., 2006). The initial system proposed by Wladimir Köppen considered the native vegetation as the best expression of climate. Köppen delineated several major climate groups according to their temperature and precipitation characteristics. The system was later refined by Rudolf Geiger, who collaborated with Köppen. The modifications incorporated a more detailed understanding of climate and its influence on vegetation (Geiger & Pohl, 1954). Previous studies have successfully used this classification system to assess CA's drying or wetting trends (Dilinuer et al., 2021; He et al., 2021). They have found the temperate continental climatic zone has been drier, while the dry, arid desert and Mediterranean continental climatic zones have been getting wetter. They suggested increasing arid and temperate zones at the expense of tundra regions, which could profoundly affect the region's ecosystems and socio-economic development.

Here, we use high-resolution gridded observation datasets and state-of-the-art future projections from two different generations of climate models to report on the spatio-temporal evolution of climate in CA. We analyse the seasonal variability of temperature in different global warming scenarios. By analysing the observations and model outputs, we report on a regime shift behaviour in the climate of CA since the beginning of the 21st century. The main five questions that we tackle are as follows:

- Has there been a noticeable trend in climate change in Central Asia over recent decades?
- What do current leading models predict for principal climate shifts in Central Asia?
- How do the latest model sets differ from previous ones in representing temperature and precipitation changes in Central Asia?
- In what ways might global warming impact seasonal temperature fluctuations in Central Asia?
- What changes in climate classification, pertinent to snow depth, are projected for Central Asia?

This study chose temperature and precipitation as critical variables to analyse recent and future climate change. First, however, to describe the impacts of climate change on the hydrological cycle, we show the trends from several additional observed climate variables. Then, we report on the spatio-temporal variability of changes for different GCMs and scenarios. Furthermore, we discuss the differences between the previous and the new model generations. Finally, we report on the seasonal cycle of climate change in CA and discuss the potential threats.

2 | DATA AND METHODS

2.1 | Observed climate

For analysing the observed climate state during the last 70 years (1950–2019), we have used the GSWP3-W5E5 observational climate input data for Inter-Sectoral Impact Model Intercomparison Project (ISIMIP) Phase 3a (ISIMIP3a; Lange, 2021). The data set is global with a horizontal resolution of 0.5° for 1901–2019 and is bias-adjusted against the W5E5 data set. W5E5 is based on version 1.0 of the WATCH data set's methodology applied to ERA5 data, WFDE5 (Cucchi et al., 2020; Weedon et al., 2014), precipitation data from version 2.3 of the Global Precipitation Climatology Project (GPCP; Adler et al., 2003) and ERA5 reanalysis data (Hersbach et al., 2020).

In order to analyse the observed dry and wet trends, we have used the self-calibrated Palmer drought severity index (scPDSI) dataset from the Climate Research Unit (ref. Table 1), which has a global coverage at a horizontal resolution of 0.5° (Diamond & Schreck, 2020; Van Der Schrier et al., 2013). The scPDSI is calculated from temperature, precipitation, and parameters related to each grid point's soil and surface characteristics. Table 1 presents the observation data this study used.

We have chosen the three climate indices introduced by Peterson et al. (2001) and an additional five variables to explore the extreme climate changes within the period of 1950–2019:

1. Number of summer days: Days in a year with a daily maximum temperature greater than 35°C.
2. Number of tropical nights: Annual number of days with a daily minimum temperature greater than 20°C.
3. Number of icing days: Annual number of days with a daily maximum temperature less than 0°C.
4. Temperature trend: The linear trend of monthly temperatures in the 1950–2019 period ($K \cdot decade^{-1}$).
5. Precipitation trend: The linear trend of monthly precipitation in the 1950–2019 period ($mm \cdot year^{-1} \cdot decade^{-1}$).

TABLE 1 Reanalysis and observation data-sets used in this study.

Variable	Data set	Time period	Source
Near-surface air temperature	GSWP3-W5E5 observational climate input data for ISIMIP3a	1901–2019	https://www.isimip.org
Precipitation	GSWP3-W5E5 observational climate input data for ISIMIP3a	1901–2019	https://www.isimip.org
Snow depth	European Centre for Medium-Range Weather Forecast (ERA5 + ERA5 back extension)	1950–1978 + 1979–2019	https://www.ecmwf.int/
Self-calibrating Palmer Drought Severity Index	Climatic Research Unit, University of East Anglia, UK	1901–2019	https://crudata.uea.ac.uk/cru/
Runoff	GRUN_v1_GSWP3_WGS84_05 IAC ETHZ	1902–2014	https://doi.org/10.5194/essd-2019-32
Glaciers	OGGM		https://oggm.org/
Köppen classification system	KG2	1981–2100	https://chelsa-climate.org/

6. Snow depth trend: The linear trend of monthly snow depth in the 1950–2019 period (mm·year^{-1}·decade^{-1}).
7. Run-off trend: The linear trend of monthly run-off in the 1950–2019 period (mm·year^{-1}·decade^{-1}).
8. scPDSI trend: The linear trend of monthly scPDSI in the 1950–2019 period (decade^{-1}).

The high resolution of observation data-sets provides us a unique opportunity to study the CA climate at a resolution of 0.5°.

To analyse the observed trends' statistical significance, we applied the Mann–Kendall trend test (Kendall, 1975; Mann, 1945). For analysis of the Köppen climate classification, we have used projections from the CHELSA (Climatologies at High resolution for the Earth's Land Surface Areas) dataset (Karger et al., 2017). The Köppen climate classification system was first formulated by the German climatologist Wladimir Köppen in the late 19th century and has undergone several modifications since. The system classifies the world's climates based on temperature, precipitation and seasonal patterns. The goal of the Köppen classification system is to facilitate the comparison of climatic zones across different regions of the world. CHELSA provides high-resolution climate data, including temperature and precipitation, crucial inputs for the Köppen classification system.

2.2 | CMIP5/CMIP6 scenarios

We have used 442 model simulations from CMIP5 and CMIP6 to evaluate the future projection trends in the CA domain. A complete list of the simulations used in this study could be found in Data S1, Supporting Information. The CA domain covers an area between the 45°E–90°E and 25°N–60°N (Figure 1). All model simulations have been remapped using the inverse distance weighting (IDW) method with a radius of 100,000 km and nine nearest neighbours for re-gridding (Lu & Wong, 2008) on the 1° resolution grid. The CMIP data set is available via the CMIP Search Interface of the World Climate Research Programme (https://esgf-node.llnl.gov/projects/, accessed on June 26, 2021).

The Representative Concentration Pathways (RCPs) are designed to represent possible future emission scenarios. The number at the end of each scenario represents the growth in radiative forcing by 2100. We refer to the study of van Vuuren et al. (2011) for a full description of the RCP scenarios. RCP scenarios used in this study are as follows:

- RCP2.6: Stabilization scenario with 2.6 W·m^{-2} radiative forcing by 2100.
- RCP4.5: "Stabilization with overshooting" with 4.5 W·m^{-2} radiative forcing by 2100.
- RCP6.0: As in RCP4.5 but with higher overshooting with 6.0 W·m^{-2} radiative forcing by 2100.
- RCP8.5: "Rising radiative forcing" scenario with 8.5 W·m^{-2} radiative forcing by 2100.

Recently quantified anthropogenic emissions for the shared socio-economic pathway (SSP) scenarios represent different future pathways based on socio-economical and political factors (Meinshausen et al., 2020). SSP scenarios used in this study are as follows:

- SSP1-2.6: One of the "high-priority" scenarios for the sixth assessment report of the Intergovernmental Panel on Climate Change (IPCC AR6). This scenario is

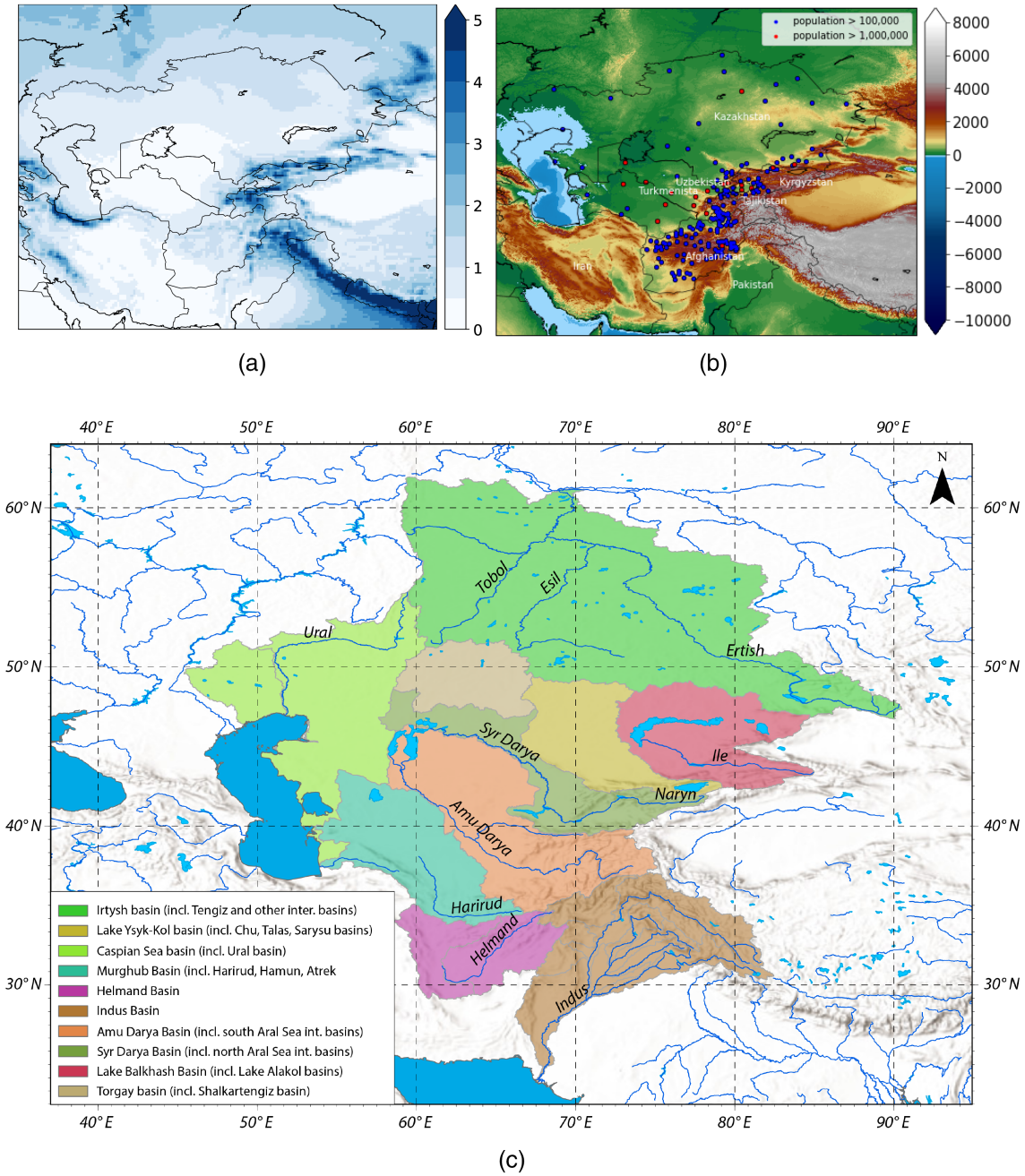

FIGURE 1 (a) Precipitation climatology from ERA5 for 1991–2020 period in mm·day^{-1}. (b) Topography map (m) from https://www.ngdc.noaa.gov/mgg/global/ and the location of cities with population greater than 100,000 (blue dots) and 1,000,000 (red dots). (c) River basins (ref. legend) in CA. Blue lines show the major rivers.

labelled as a "2°C" scenario and is among the "sustainability" SSP1 socio-economic category with a radiative forcing of 2.6 W·m^{-2} in the year 2100.

- SSP2-4.5: SSP2 scenario is labelled as "a Middle of the road" scenario, and SSP2-4.5 is an update of the RCP4.5 and represents the medium pathway. It assumes climate protection strategies are being taken. The world's population is assumed to level off in the second half of the century, with a moderate increase in the first half.
- SSP3-7.0: A "regional rivalry" scenario where the world faces rising inequality. Drastic environmental damages will occur on regional scales. In this scenario, the radiative forcing will reach 7.0 W·m^{-2} in the year 2100.
- SSP5-8.5: Or, the so-called "Fossil-fueled Development" scenario assumes a world with a growing economy which is based on fossil fuel consumption (high percentage of coal) with a radiative forcing of 8.5 W·m^{-2} in the year 2100.

3 | RESULTS

3.1 | Observed climate extremes

Kyrgyzstan and Tajikistan, characterized by cold and cold snow-forest climate types (E and D), receive most of the yearly precipitation in CA (Figure 1b). Such precipitation fills the water storage of river basins of three major rivers in CA: Syr Darya, Amu Darya and Irtysh River (Yang et al., 2020). Figure 1 indicates that the highly populated cities are located near major rivers or regions with a large amount of yearly precipitation (elevated regions in CA). Most CA cities with a population of over 1 million and a large portion of yearly precipitation are located in the Amu Darya and Syr Darya basins. Their freshwater originates from the mountains of Tajikistan and Kyrgyzstan via snow/glaciers melting in warmer seasons. Therefore, the elevated area in the East of CA plays a critical role in water security in the entire area.

3.1.1 | Temperature trends

Temperature is one of the most sensitive variables to anthropogenic forcing and is one of the critical indicators in climate change studies. The linear warming trend in CA for the 1950–2019 period is shown in Figure 2. The entire CA domain shows a positive warming trend. More significant warming trends exist over the west and southwest of Afghanistan, the Aral Sea and Kyrgyzstan. The temperature anomalies (w.r.t. 1950–1979 period) show that during the last 20 years, colder months are warming higher than warmer months (Figure 2b). This will expressly stress the glaciers and water storage regions in

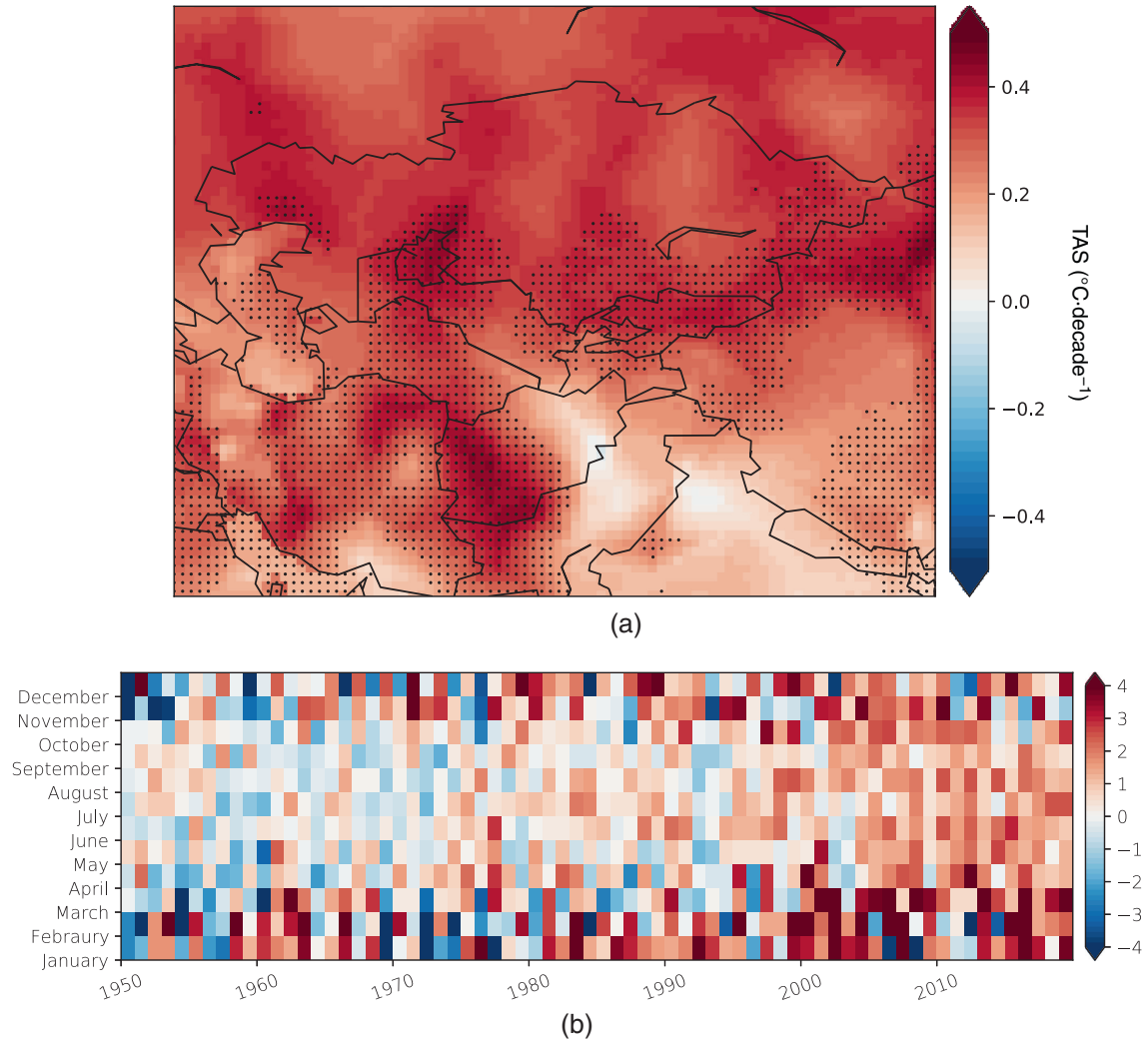

FIGURE 2 (a) Temperature trends (°C·decade^{-1}) during the 1950–2019 and (b) Central Asian monthly temperature anomalies with respect to the 1950–1979 mean. The dots in (a) indicate the grid-points with a significant trend with p-value <0.05 using the Mann–Kendall significance test. Data is from GSWP3-W5E5 (Table 1).

mountainous areas in CA. The monthly temperature in June and August has never been less than the mean value for the 1950–1979 reference period since 2004 (15 consecutive years). However, the warming during September will extend the glacier's shrinkage period and contribute to more river discharge. This will be critical for the CA countries if they do not adapt to future abrupt river discharge increases.

3.1.2 | Hydro-climatological trends

To analyse the consequences of such warming on the observed hydro-climatic situation in CA, we create maps of several climate indices (ref. section 2) and trends of critical variables. Figure 3a–d presents the trends in precipitation, snow depth, runoff and scPDSI from 1950 to 2019. By increasing temperatures in CA, the precipitation trend shows an overall increase in the CA countries (Figures 3b, 4b and 5). The maximum trend appears in East Afghanistan. This pattern is an artefact found in the GSWP3-W5E5, GPCC and W5E5v2.0 datasets (not shown here). There exists a decreasing precipitation trend over Tajikistan and west Kyrgyzstan (not significant). However, a consequence of the warming trend is the snow depth deficit in CA, especially over mountainous areas of Tajikistan, Kyrgyzstan and Afghanistan (Figure 3c), a region with a large portion of CA glaciers (Figure 3h). The snow depth time series over the entire CA region shows a significant decline since 1970 with 6 mm·month^{-1} for 1.24°C warming (Figure 4a). Increasing precipitation, temperature and snow-melt increase runoff over East Afghanistan and North Kazakhstan. This might contribute to an increase in flash floods in these regions. However, the runoff declines over CA glaciers. As an extra measure of hydro-climatic changes, we show the scPDSI trends in Figure 3d.

The scPDSI is a widely recognized metric used to measure the severity of drought conditions based on long-term historical weather data. It is an enhancement of the original Palmer Drought Severity Index (PDSI), which was introduced by Wayne Palmer in the 1960s (Palmer, 1965). The PDSI is designed to reflect the cumulative deficits in soil moisture, taking into account recent weather patterns, including temperature and precipitation, along with the local water balance, involving evaporation, transpiration, runoff and soil moisture capacity. The scPDSI improves upon the original PDSI by incorporating a self-calibrating feature that adjusts the time scale of the index to fit the local climate better, making it more universally applicable across different regions with varying climatic conditions. This adjustment is crucial because it allows the scPDSI to more accurately reflect drought conditions in areas with distinct climate patterns without being biased by the climatic assumptions inherent in the original PDSI formula.

Our analysis of scPDSI shows that there exists a tendency for wetter conditions over North Kazakhstan and East Afghanistan and for drier conditions over vulnerable areas of Central Kazakhstan, Southwest Afghanistan (the boundary between Iran, Afghanistan and Pakistan), and large areas of Turkmenistan. The Number of summer days and tropical nights increased by more than 10 days per year in the 1990–2019 period concerning the 1950–1979 period over the regions with maximum drying trends (Figure 3e,f). There exists a homogeneous decrease in the Number of icing days (more than 15 days per year) in CA, which is vital for stabilizing the water storage in mountainous areas (Figure 3g).

3.1.3 | Precipitation–temperature relationship

To highlight the fundamental relationship between temperature and precipitation in CA and understanding how these two crucial climate variables interact with each other, we show the bivariate plot of temperature and precipitation over CA (Figure 7). Since temperature can significantly influence the hydrological cycle, understanding this relationship is essential for grasping how warming trends may affect precipitation patterns.

The slope of the linear trend is 0.05. Therefore, any warming will increase the precipitation by 0.05 mm·day^{-1}. The following section shows that the same slope exists in future model simulations from CMIP model ensembles. By quantifying the relationship with a slope value (0.05 mm·day^{-1} per degree of warming), we provide a specific measure of sensitivity that can be used for further analysis. This kind of quantitative insight is invaluable for predictive models and for understanding the potential impacts of climate change. Establishing the current relationship between temperature and precipitation sets a baseline against which future model projections can be compared (section 3.2.2).

3.1.4 | Köppen classification

The map in Figure 6 displays the Köppen climate classification for the CA region for the period 1981–2010. As depicted on the map, CA showcases a diversity of climate zones, reflecting the complex interplay between geography and climate. Table 2 describes the climate categories of the Köppen system. In the Köppen system, the "A" climates represent tropical climates, which are typically not

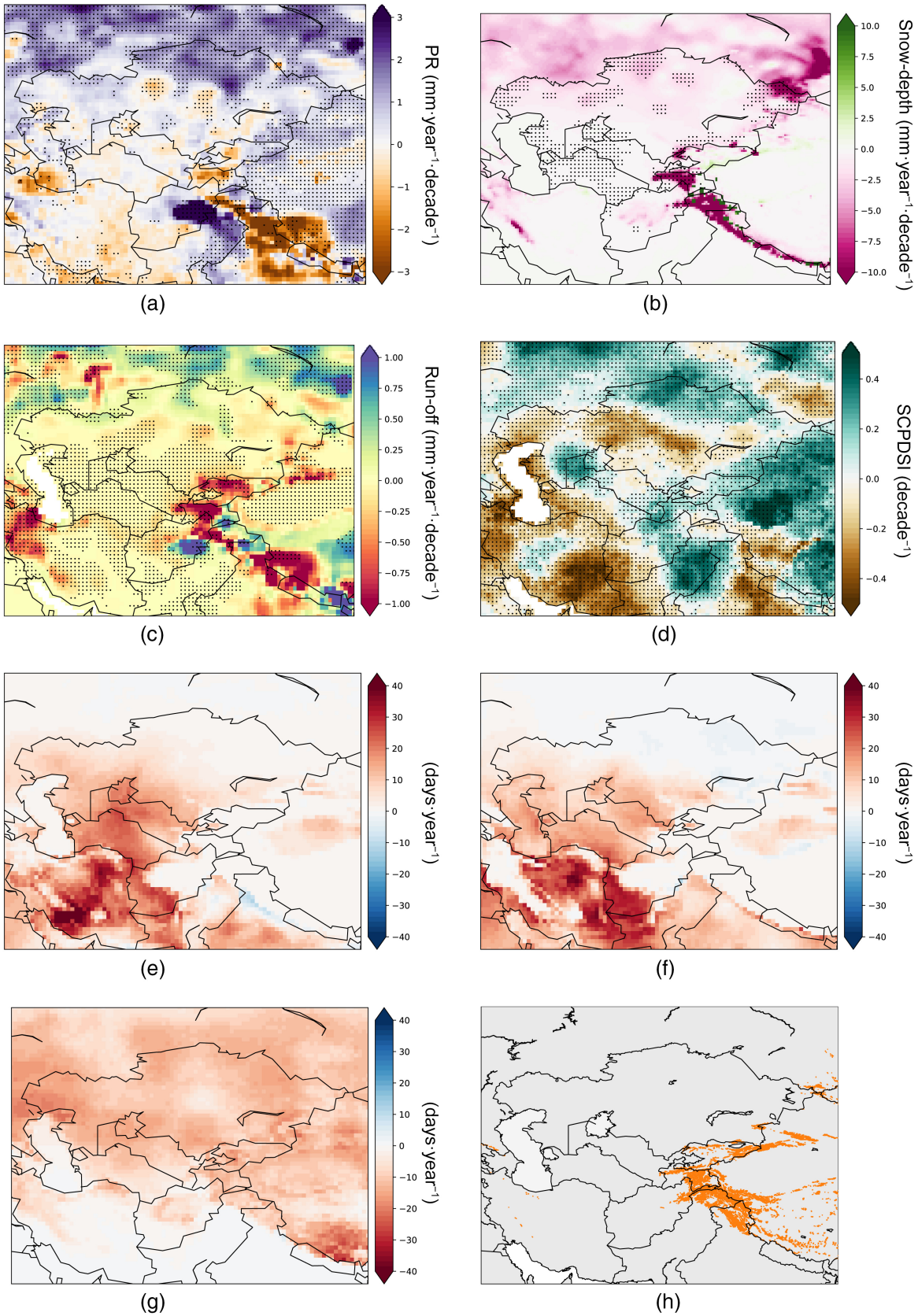

FIGURE 3 Trends in precipitation (a), snow depth (b), run-off (c) and scPDSI (d) for the 1950–2019 period. Changes in summer days (e), tropical nights (f) and icing days (g) between the 1990–2019 and 1950–1979 periods. Glaciers' location are shown in (f). The dots in the maps indicate the grid-points with a significant trend with p-value <0.05 using the Mann–Kendall significance test. For the list of data used for visualization we refer to Table 1.

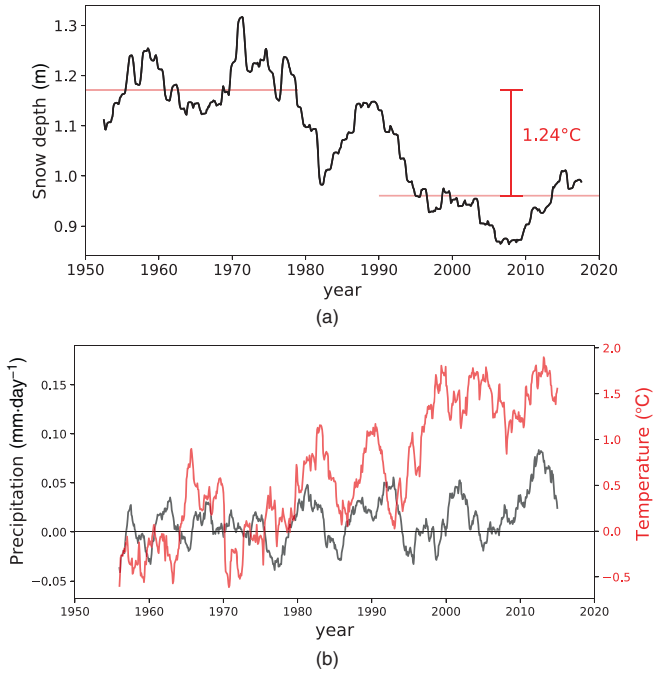

FIGURE 4 (a) Five-year running mean of snow depth time-series over CA. (b) Five-year running mean of precipitation and temperatures over CA.

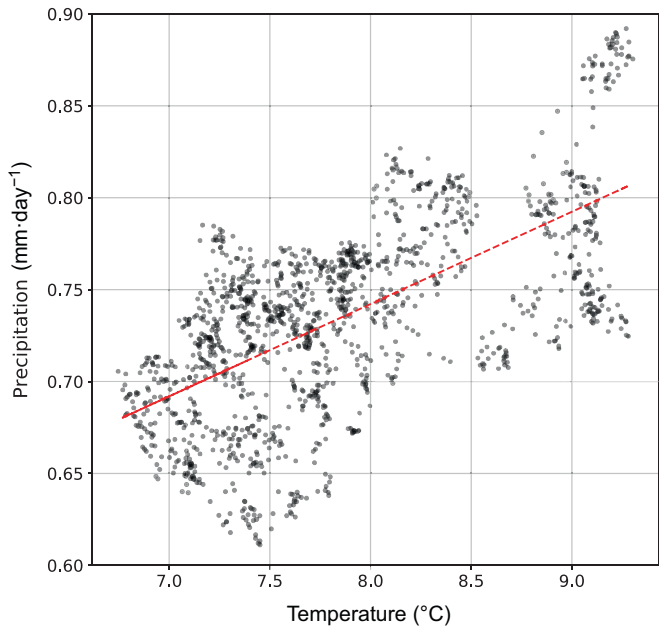

FIGURE 5 Bivariate plot of temperature and precipitation over CA. The dashed red line indicates the linear fit ($pr = 0.05 \times tas + 0.34$).

the dominant climates in CA due to the region's distance from the equator and its high average elevations. The more prominent climate categories in CA tend to be "B" (Arid and Semi-arid), "C" (Temperate) and "D" (Cold), along with some "ET" (Tundra) at the highest elevations. "BWk" (Cold desert) and "BWh" (Hot desert) climates are particularly important, reflecting the region's vast arid and semi-arid zones, including some of the world's largest deserts. These areas receive very little precipitation and experience high-temperature variability. The "BSk" (Cold steppe) and "BSh" (Hot steppe) climates are also significant, representing areas with more precipitation than deserts but still insufficient for most trees to grow, leading to grassland vegetation. In the temperate "C" climate zones, such as "Cfb" (Warm temperate, fully humid warm summer) and "Csa" (Warm temperate summer, dry, hot summer), which might be found in the more moderate climatic regions of CA, there are warmer and wetter conditions compared to the arid "B" climates.

The map effectively illustrates the variety of climates that can be found across CA. This region spans a considerable latitudinal range and contains various topographical features, including high plateaus, vast deserts and significant mountain ranges. The climate categories indicated by the Köppen system provide insights into the ecological and agricultural potential of the region, as well as challenges such as water scarcity and extreme temperatures.

3.2 | Future projections

3.2.1 | Temporal changes

Figure 7 presents the temperature and precipitation anomaly projections from CMIP5 and CMIP6 model simulations. Here, we show the average monthly mean temperature anomalies over the central Asian region for the above scenarios with 442 model simulations. The entire region shows an increase in annual temperatures in all scenarios, ranging from ~2 to ~6°C concerning the 1976–2005 reference period. The monthly precipitation increases accordingly. Around 2030, the scenarios start to diverge and follow the path of four utterly different climate states in both CMIP simulation sets. CMIP6 simulations show warmer and wetter trends than CMIP5 at the end of the century. The observed trends of temperature changes (black line in Figure 7a,b) is well captured by the CMIP5 and CMIP6 ensemble means during the historical period. For precipitation, the observation trend stay in the range of climate model simulations for the historical period.

3.2.2 | Spatial changes

Figures 8 and 9 depict the spatial maps of the averaged temperature and precipitation changes for the end of the

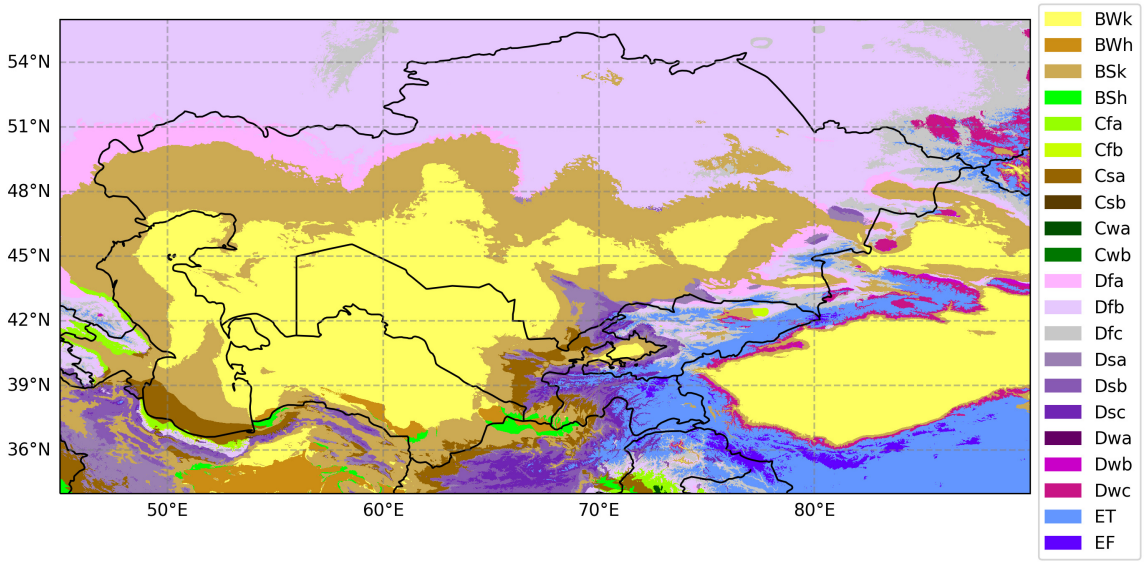

FIGURE 6 Köppen classification map in Central Asia from the CHELSA dataset for 1981–2010.

century (2071–2100) for the two different CMIP simulation sets. The entire CA domain shows an increase in temperature and precipitation in both sets. The main difference in patterns of precipitation change in CA between the CMIP5 and CMIP6 appears in Afghanistan. The CMIP5 simulations indicate a drying trend in contrast to CMIP6. Higher radiative forcing scenarios (SSP3-7.0 and SSP5-8.5) of CMIP6 present unique warming patterns in CA, even comparable with the RCP8.5. The temperature change patterns of both scenarios might be of concern in CA, especially over vulnerable highlands with glaciers. We have to note that the precipitation change values show high model agreement over CA, except over Iran and some parts of Afghanistan, and the patterns of temperature change show high model agreement over CA (Data S1).

As seen in the observation period (Figure 5), a very similar linear relationship between the temperature and precipitation anomalies exists among the 442 model simulations (Figure 10a,b). This indicates that the CMIP models maintain the observed precipitation–temperature relationship for future scenarios.

While both sets of models show a trend of increasing temperature and precipitation with higher emission scenarios, CMIP6 generally predicts a more significant temperature increase for the higher scenarios. In contrast, CMIP5 shows a more substantial initial increase in precipitation under the low-emission scenario (RCP2.6) compared to CMIP6's SSP1-2.6. The relatively modest increases in precipitation compared to temperature rise could suggest that the region might face increased water stress, as higher temperatures can enhance evaporation rates, potentially offsetting the slight increases in precipitation. The differences in temperature and precipitation changes between CMIP5 and CMIP6 highlight the importance of continuously refining climate models to better capture the complexities of regional climates.

3.2.3 | Seasonal temperature cycles

Figure 11 shows the seasonal cycles of temperature and precipitation changes from CMIP5 (RCP2.6 and RCP8.5) and CMIP6 (SSP1-2.6 and SSP5-8.5) for three different time-slices of near-future (2011–2040), Mid-century (2041–2070) and far-future (2071–2100) concerning 1976–2005 reference period. There is a good agreement between the CMIP5 and CMIP6 models for temperature changes in the near-future time-slice with an ensemble mean of 2°C. However, the uncertainty range exceeds the 3°C. This warming leads to an increase of 0.1 mm·day^{-1} in precipitation in CA (Figure 11b) throughout the year.

For the middle of the century, the uncertainty range of the ensembles almost doubles (Figure 11c,d). However, the ensemble means between the CMIP5 and CMIP6 are not significantly different. The differences between the CMIP5 and CMIP6 models are more apparent in the far-future period (Figure 11e,f). The uncertainty range of the CMIP5 ensemble for the RCP8.5 is smaller than the CMIP6-SSP5-8.5. One reason might be the smaller Number of ensemble members from CMIP6 (46 models) than the CMIP5 (89 models). However, both CMIP model ensembles indicate a warming of 6°C with a minimum uncertainty range of 6°C throughout the year

TABLE 2 Köppen climate classification mapping after (Peel et al., 2007).

Code	Climate classification
1	Af—Equatorial fully humid
2	Am—Equatorial monsoonal
3	As—Equatorial summer dry
4	Aw—Equatorial winter dry
5	BWk—Cold desert
6	BWh—Hot desert
7	BSk—Cold steppe
8	BSh—Hot steppe
9	Cfa—Warm temperate fully humid hot summer
10	Cfb—Warm temperate fully humid warm summer
11	Cfc—Warm temperate fully humid cool summer
12	Csa—Warm temperate summer dry hot summer
13	Csb—Warm temperate summer dry warm summer
14	Csc—Warm temperate summer dry cool summer
15	Cwa—Warm temperate winter dry hot summer
16	Cwb—Warm temperate winter dry warm summer
17	Cwc—Warm temperate winter dry cool summer
18	Dfa—Snow fully humid hot summer
19	Dfb—Snow fully humid warm summer
20	Dfc—Snow fully humid cool summer
21	Dfd—Snow fully humid extremely continental
22	Dsa—Snow summer dry hot summer
23	Dsb—Snow summer dry warm summer
24	Dsc—Snow summer dry cool summer
25	Dsd—Snow summer dry extremely continental
26	Dwa—Snow winter dry hot summer
27	Dwb—Snow winter dry warm summer
28	Dwc—Snow winter dry cool summer
29	Dwd—Snow winter dry extremely continental
30	ET—Polar tundra
31	EF—Polar frost

(Figure 11e). That range of warming in June–September will contribute to extended shrinkage of the glaciers. On the other hand, the increase in precipitation during the winter contributes to snow/ice storage in the region. However, the community should further study the combination of these phenomena.

It has been shown that in CA, the snow/glacier's melting contributes to the rivers' flow and secures the region's water availability (Didovets et al., 2021). Therefore, such a significant temperature shock will stress the hydrological cycle and contribute to the instability of water security in the vulnerable CA regions in the upcoming decade. Under sustainable paths (RCP2.6 and SSP1-2.6), the temperature change levels will remain at 2°C during all the time-slices and throughout the year.

3.3 | Changes in Köppen classification

The Köppen climate classification is a widely used system for classifying the world's climates based on the average and typical ranges of different climate variables, most commonly temperature and precipitation (Karger et al., 2017). We have used projections from the CHELSA (Climatologies at High resolution for the Earth's Land Surface Areas) dataset, which is known for providing high-resolution climate data (Karger et al., 2017, 2021, 2023). CHELSA is often used in ecological modelling and biodiversity research due to its fine spatial resolution and reliability.

The top 20 changes in the number of grid points from one to another Köppen category in CA, as shown in Figures 12 and 13 for different SSPs and time slices, can indicate shifts in the regional climate characteristics over time. We analysed the projected changes in Köppen climate categories over CA for three different SSPs and two time slices: 2041–2070 and 2071–2100. These time slices aim to provide a mid-century and end-of-century view of climate projections:

- Middle of the century (2041–2070): SSP126: This scenario is often considered a "sustainability" pathway that assumes significant mitigation efforts to limit warming. The transitions here may suggest moderate changes towards warmer climates but emphasize maintaining current climate zones where possible. SSP370: Represents a "middle of the road" pathway where some efforts at mitigation are made, but not stringently. The transitions under this scenario might show more pronounced shifts towards warmer and drier climates than SSP126, reflecting less aggressive mitigation efforts. SSP585: This is a high-emission scenario without significant climate change mitigation efforts, often leading to more drastic changes. The transitions could show significant shifts to much warmer climate classifications, suggesting extensive warming and drying, especially in currently cold climates.
- End-of-century (2071–2100): SSP126: For this later period, even under a sustainability scenario, the changes become more pronounced than in the earlier period, potentially reflecting the inertia in the climate system where earlier emissions continue to have effects. SSP370: This could show an acceleration of climate zone changes as the cumulative effects of

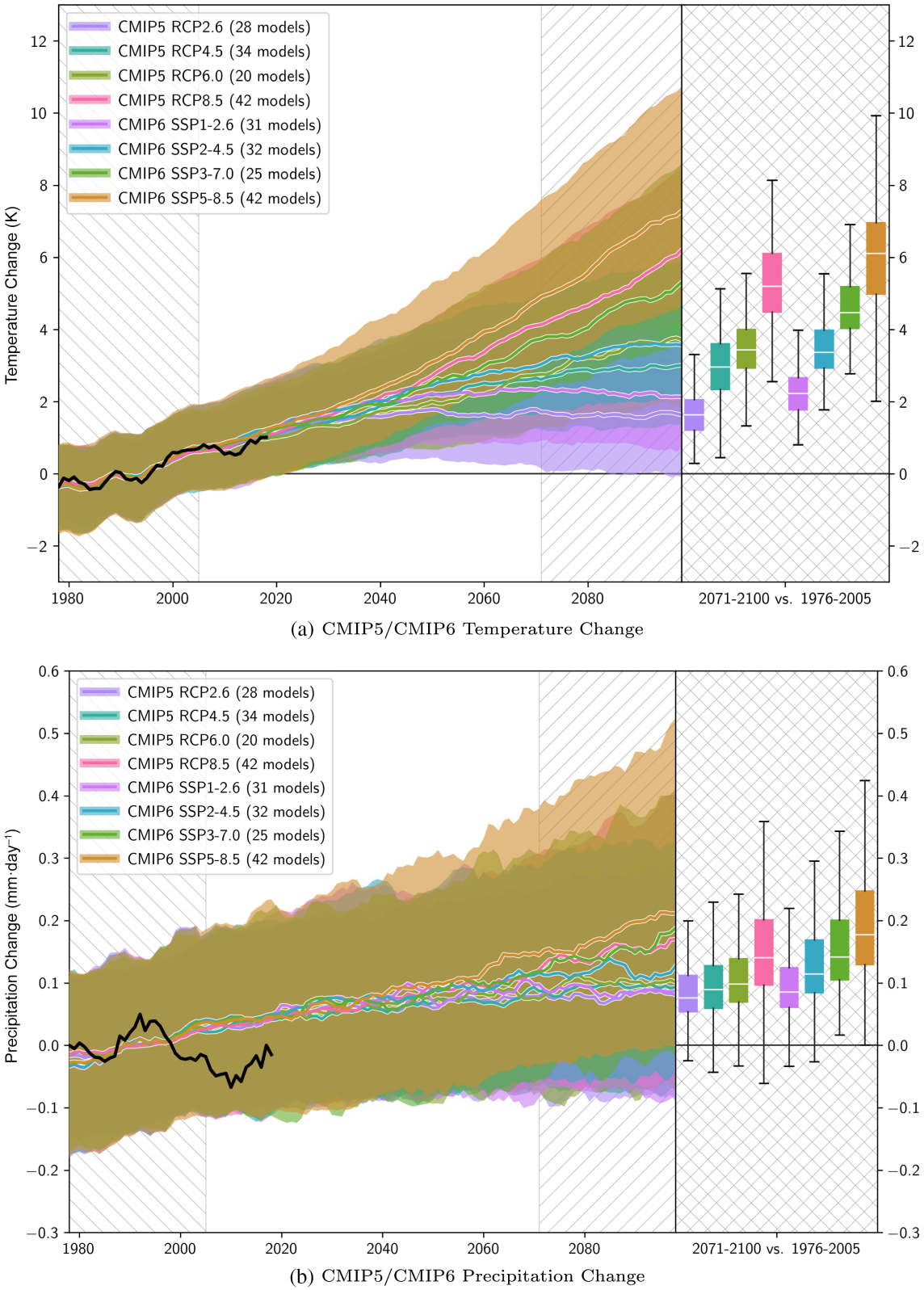

FIGURE 7 Temperature (a) and precipitation (b) changes over Central Asia (red box in Figure 8) w.r.t. reference period of the 1976–2005 for CMIP5 and CMIP6. Shadings show the models' uncertainty band. The black lines show the observed time-series.

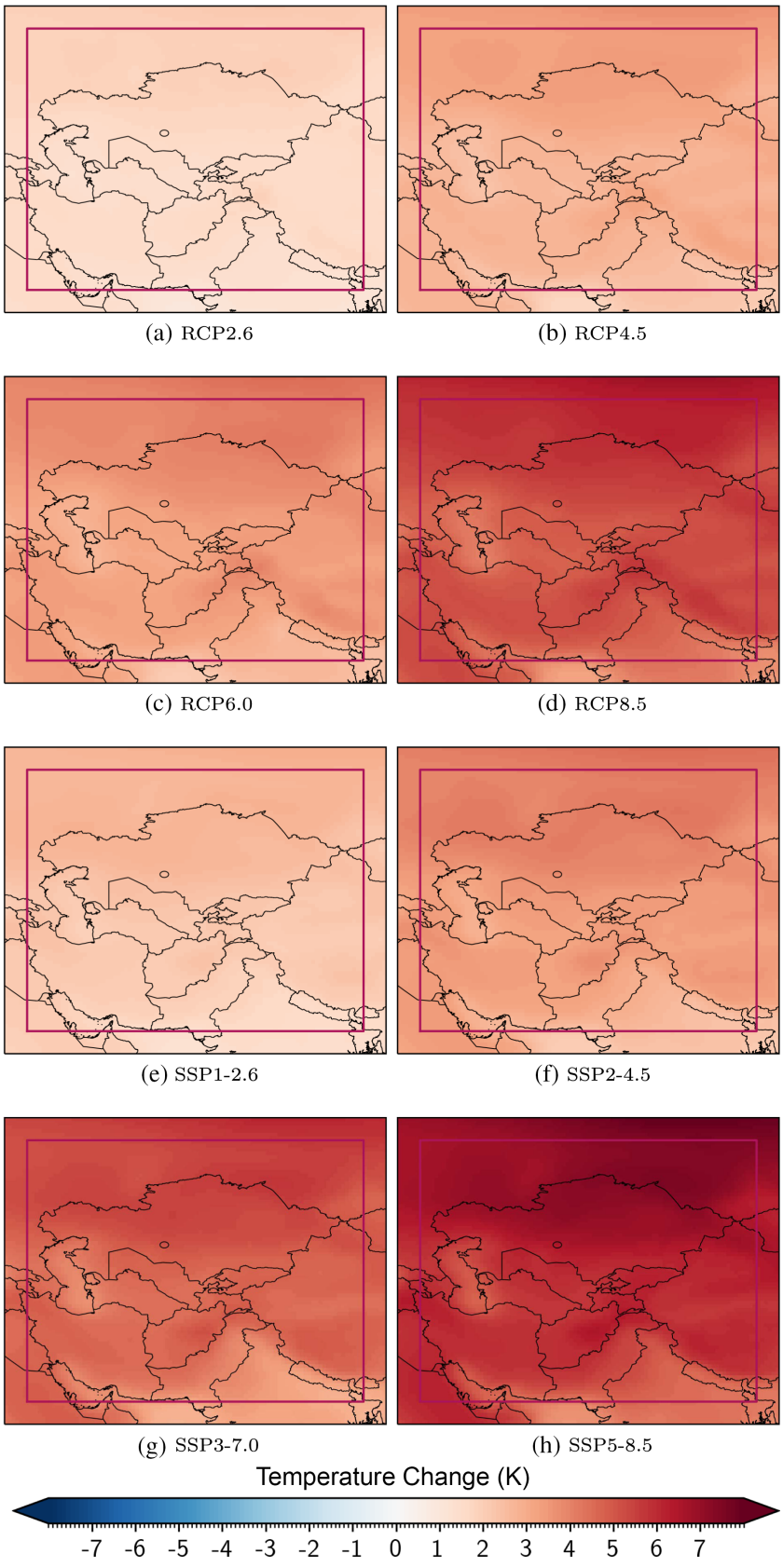

FIGURE 8 Maps of temperature change (°C) for the end of the century (2071–2100) from four different scenarios of CMIP5 (a–d) and CMIP6 (e–h). The changes are calculated with respect to the period 1976–2005. The dark red box indicates the Central Asian box over which the time-series (Figures 7, 10 and 11) are calculated.

greenhouse gas emissions manifest more strongly. SSP585: Expected to show the most dramatic transitions as the full impact of high emissions intensifies. Regions may experience significant shifts from cold and temperate climates to warmer ones, profoundly impacting ecosystems and human systems.

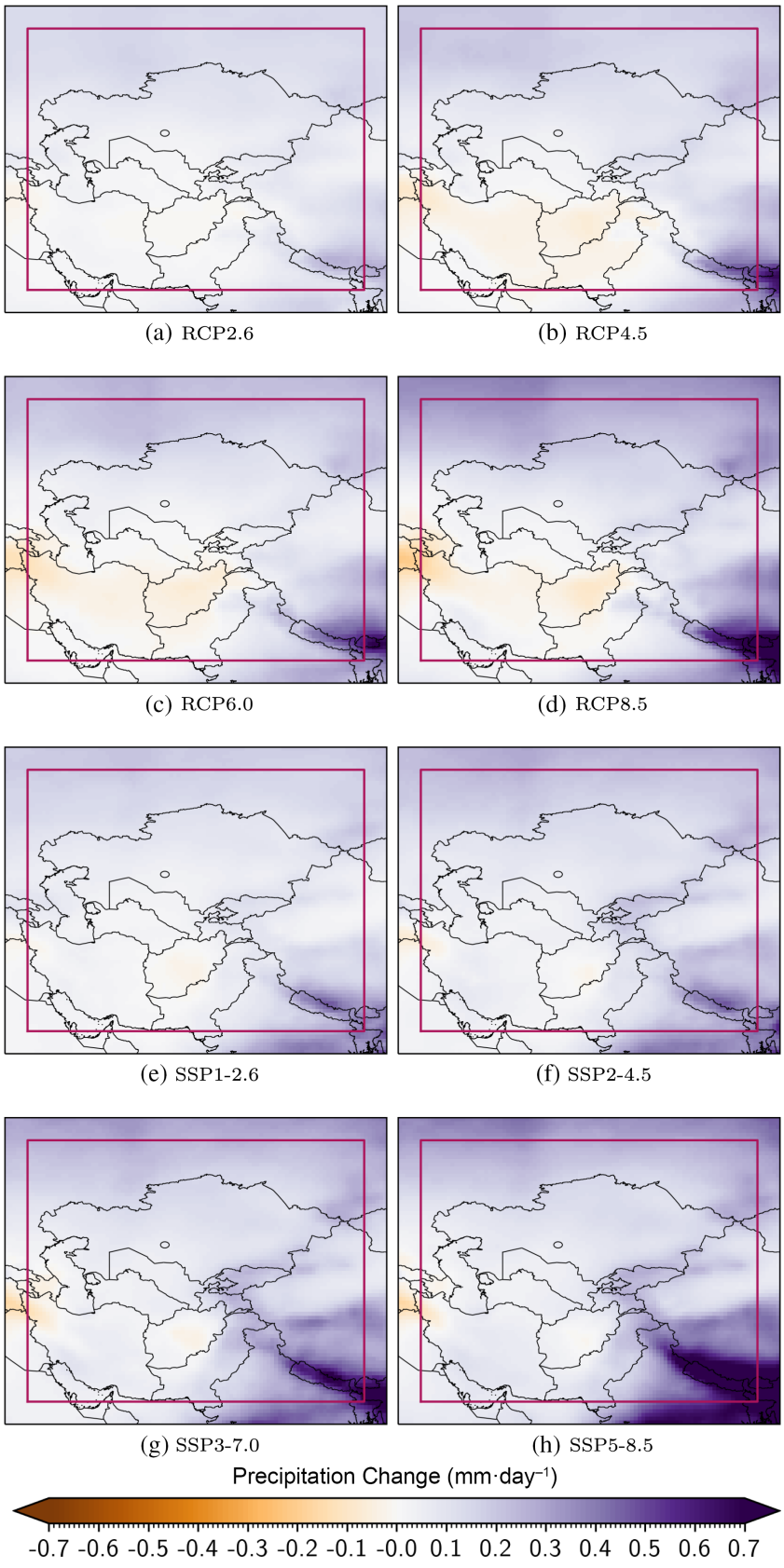

FIGURE 9 Maps of precipitation change (mm·day^{-1}) for the end of the century (2071–2100) from four different scenarios of CMIP5 (a–d) and CMIP6 (e–h). The changes are calculated with respect to the period 1976–2005. Dark red box indicates the Central Asian box over which the time-series (Figures 7, 10 and 11) are calculated.

The general trend indicates a shift towards warmer climate classifications for both time slices. This could mean that areas currently experiencing cold winters (Dfb) may transition to milder winters (Dfa), and semi-arid regions (BSk) may become more arid (BWk). It is important to note that these changes could have

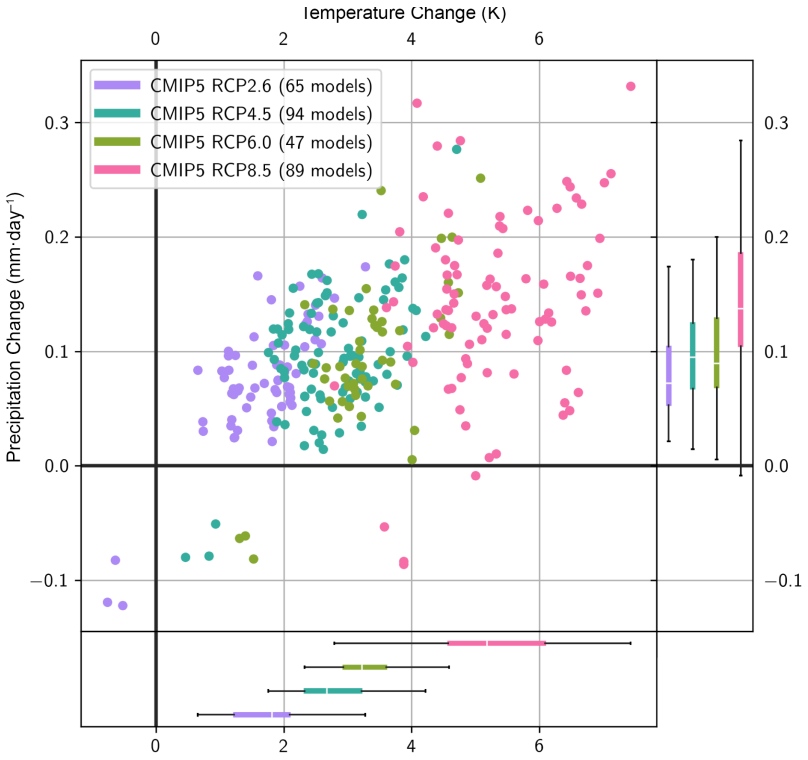

(a) CMIP5

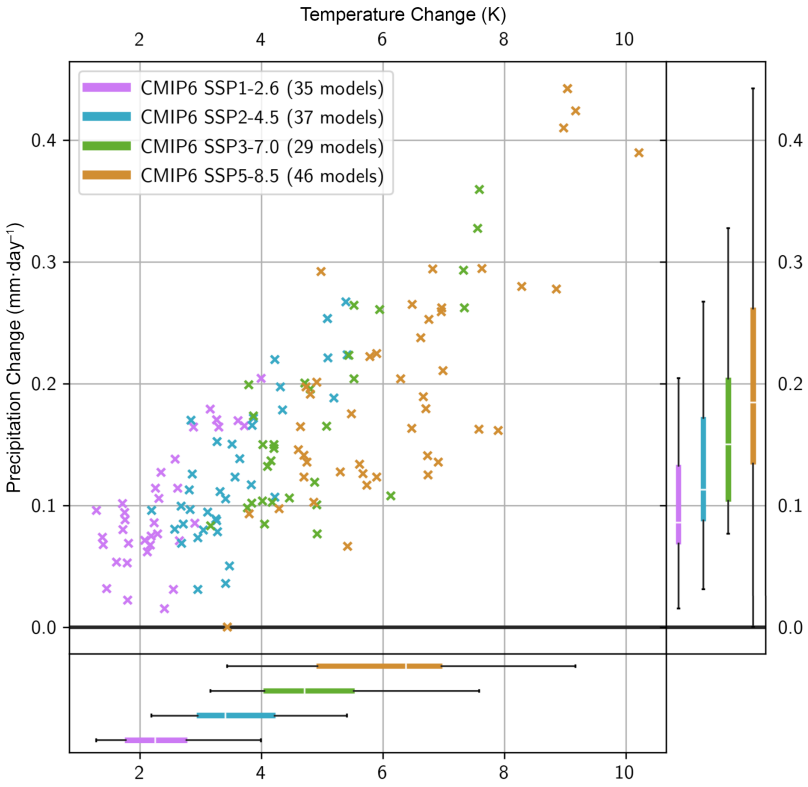

(b) CMIP6

FIGURE 10 Bivariate variable plot of precipitation and temperature changes in the 2071–2100 period w.r.t. the 1976–2005 reference period for (a) CMIP5 and (b) CMIP6. Circles and crosses represent the CMIP5 (295 runs) and CMIP6 (147 runs) models, respectively.

significant ecological and socio-economic impacts, as they may alter the distribution of biomes, affect agricultural zones and lead to changes in water availability and human health. The most drastic changes, particularly under SSP585, suggest a need for urgent and comprehensive climate action to mitigate the impacts of such

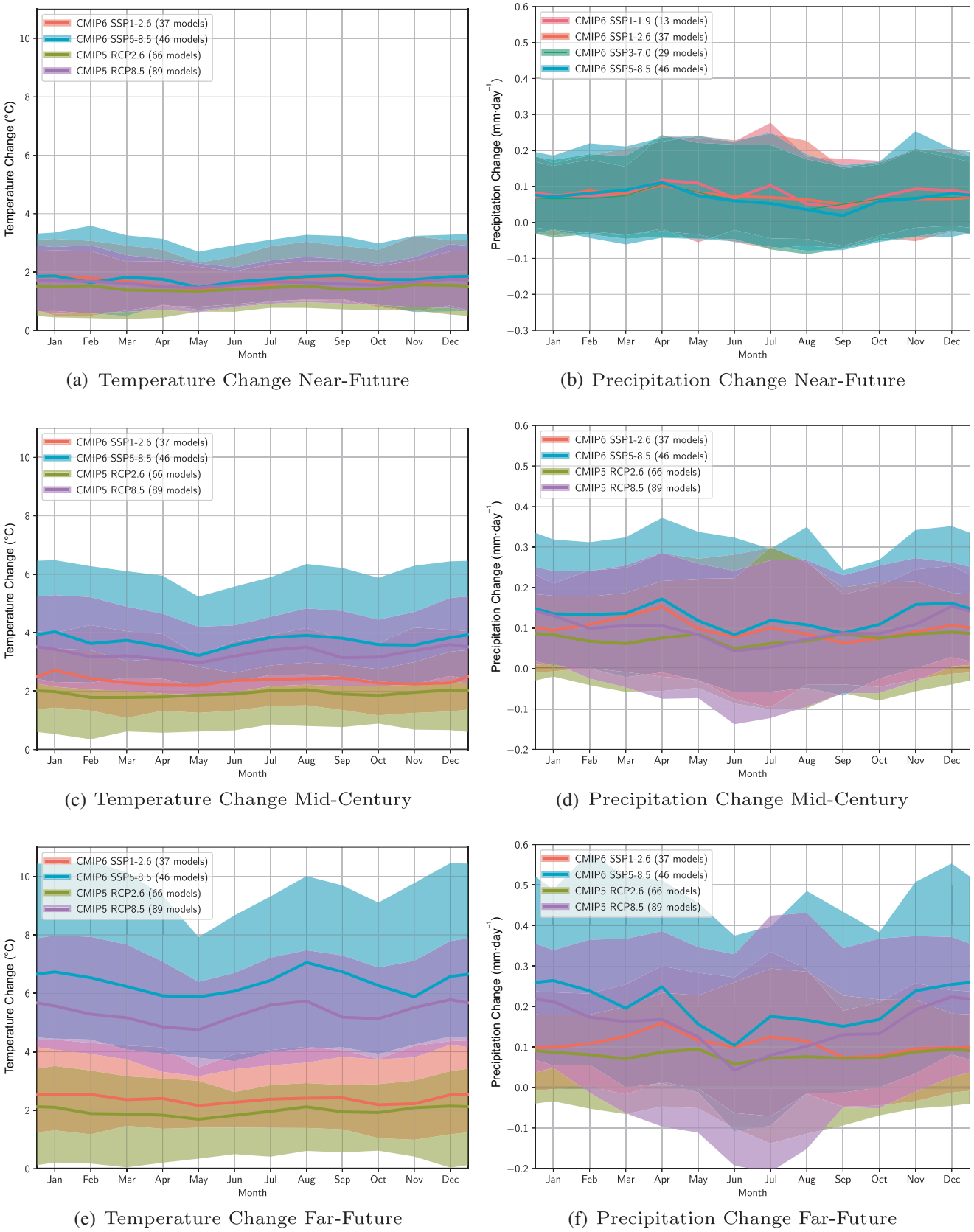

(a) Temperature Change Near-Future

(b) Precipitation Change Near-Future

(c) Temperature Change Mid-Century

(d) Precipitation Change Mid-Century

(e) Temperature Change Far-Future

(f) Precipitation Change Far-Future

FIGURE 11 Seasonal cycle of temperature (a, c, e) and precipitation (b, d, f) changes from CMIP5 and CMIP6 in the near-future (2011–2040), middle of the century (2041–2070) and far-future (2071–2100) period w.r.t. the 1976–2005 reference period. The bold lines show the ensemble mean.

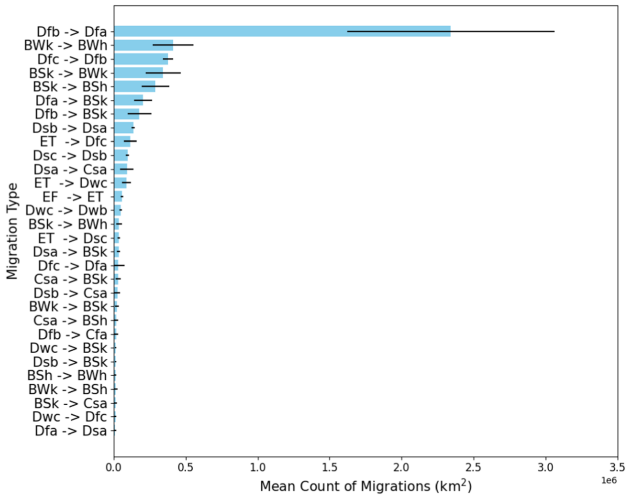

(a) ssp126

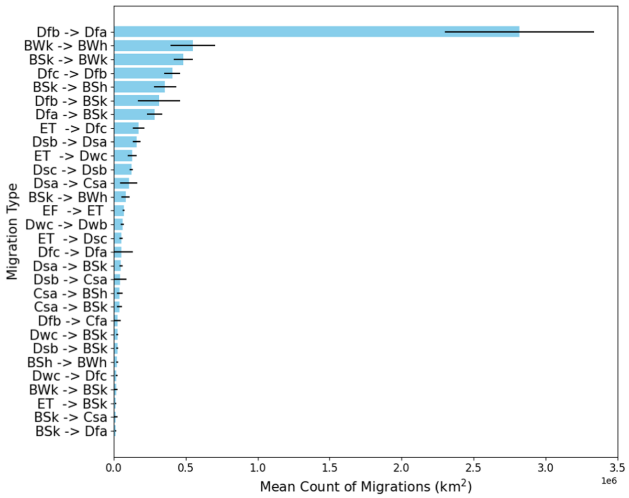

(b) ssp370

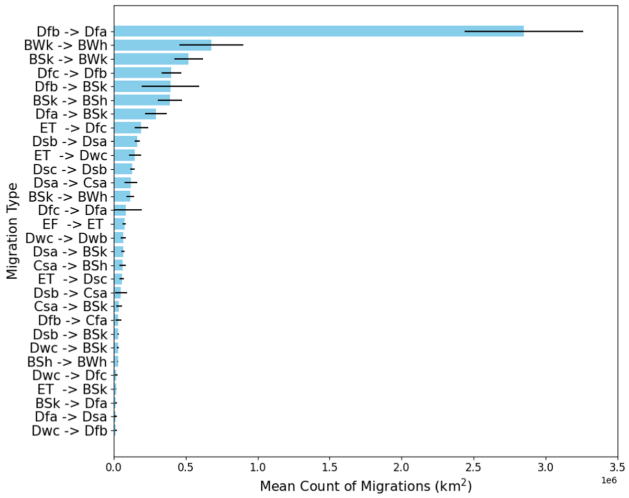

(c) ssp585

FIGURE 12 Top 20 migrations of Köppen climate categories for the middle of the century (2041–2070). Black lines present the standard deviation among the five models (GFDL-ESM4, IPSL-CM6A-LR, MPI-ESM1-2-HR, MRI-ESM2-0 and UKESM1-0-LL). Note that the *x*-axis has factor of 1e6.

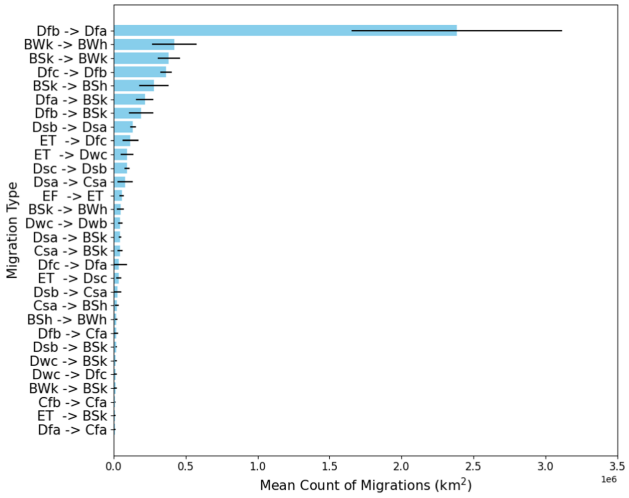

(a) ssp126

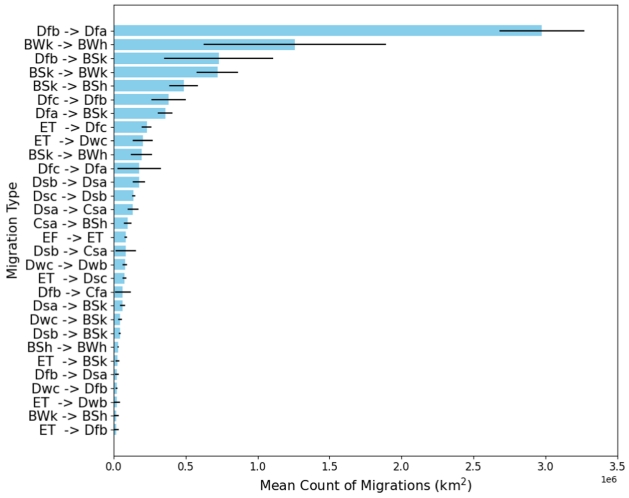

(b) ssp370

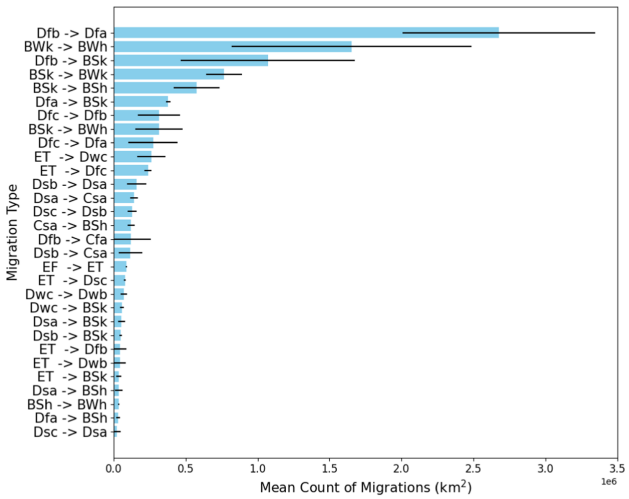

(c) ssp585

FIGURE 13 Top 20 migrations of Köppen climate categories at the end of the century (2071–2100). Black lines present the standard deviation among the five models (GFDL-ESM4, IPSL-CM6A-LR, MPI-ESM1-2-HR, MRI-ESM2-0 and UKESM1-0-LL). Note that the *x*-axis has factor of 1e6.

transitions. The data points towards a potential future where adaptive strategies become increasingly critical for sustaining biodiversity, ensuring water security and maintaining agricultural productivity. The main climate categories' migrations in CA are listed below:

- Dfb to Dfa migration: This migration appears to be the most prominent across all scenarios and periods. It suggests a significant shift from a colder snow climate with significant precipitation year-round (Dfb) to a warmer snow climate (Dfa). This could indicate a warming trend in regions that traditionally have frigid winters.
- BWk to BWh migration: This transition is common across scenarios, indicating a shift from cold desert climates (BWk) to hot desert climates (BWh). This could have major implications for water availability, agriculture, and biodiversity as regions become hotter and drier.
- BSk to BWk and Dfc to Dfb migrations: These migrations represent a transition from a steppe climate (BSk) to a cold desert climate (BWk) and from a subarctic climate with cool summer and extreme winter (Dfc) to a subarctic climate with moderate summer (Dfb), respectively. These changes suggest an expansion of desert conditions and warming of cold regions, which could affect ecosystems and human habitation patterns.
- EF to ET migration: This shift from ice cap climate (EF) to tundra climate (ET) is less frequent but still significant, indicating a potential retreat of ice cap regions, allowing for more tundra-like conditions. This change is especially poignant as it marks a possible reduction in areas currently covered by ice, with broad impacts on sea level, albedo and global climate patterns.

These observed transitions could lead to drastic changes in local and regional climates, potentially impacting agriculture, water resources, biodiversity and human livelihoods. The overall trend suggests a warming scenario where colder climates become warmer and drier climates expand. The impact of these changes would likely be complex, requiring detailed regional studies to understand the consequences and develop adaptation strategies fully.

3.3.1 | Climate impacts on Central Asia

The observed shifts in climate categories across these scenarios and time slices suggest several impacts: Water Resources: CA relies heavily on glacial melt for its water supply. Reducing snow-climate categories could significantly impact water availability, affecting agriculture, hydropower and human consumption. Agriculture: Transition to hotter and drier climates necessitates changes in agricultural practices, crop varieties and irrigation methods. Ecosystems: Biodiversity may be at risk due to shifts in climate zones. Some species may be unable to adapt to the rapid changes, leading to reduced biodiversity. Human Health: heat waves could have severe implications for public health if their frequency and intensity is increased, especially among vulnerable populations. Economic Impacts: As agriculture adapts to changing climates, there may be economic shifts, with some regions facing reduced productivity and others finding new opportunities. It is important to note that while SSPs provide a framework for projecting future changes, the actual impacts will depend on numerous factors, including local adaptation measures, technological advancements and unforeseen social and political developments. Detailed, region-specific studies would be required to understand the precise implications of these climate projections.

3.3.2 | Syr Darya and Amu Darya

In the Köppen climate classification system, the category that includes glaciers, perpetual snow, and areas of significant snow cover is designated as the "E" climate type. The "E" climates are primarily characterized by their extremely cold temperatures throughout the year. Within this category, there are two main subcategories:

- ET (Tundra Climate): This climate type is found on the edges of the ice cap climate, regions with the mean temperature of the warmest month below 10°C but above 0°C. In these areas, the ground is permanently frozen (permafrost), but the surface thaws sufficiently to support low-growing vegetation during the brief summer.
- EF (Ice Cap Climate): This is the climate of the polar ice caps. The EF climate is characterized by temperatures that do not rise above 0°C in any month of the year, meaning that all precipitation falls as snow and ice covers the ground year-round. This category includes the interiors of Greenland and Antarctica, where permanent ice and snow are present.

Figure 14 compares the changes in the tundra (ET) and ice cap (EF) categories over two significant rivers of CA, that is, Amu Darya and Syr Darya for SSP585 scenario and at the end of the century. Across all model simulations for the SSP585 scenario, there is a marked reduction in the extent of ET and EF categories

compared to the historical period. This reduction suggests a significant warming trend in these regions, with areas previously characterized by ET and EF climates transitioning to warmer climate types. Despite the differences in each climate model, there is a consistent reduction pattern in the ET and EF categories. This consistency underscores the robustness of the projected warming signal in these high-latitude/high-altitude zones. The presence of less snow and ice cover in future scenarios, as indicated by the reduction of ET and EF

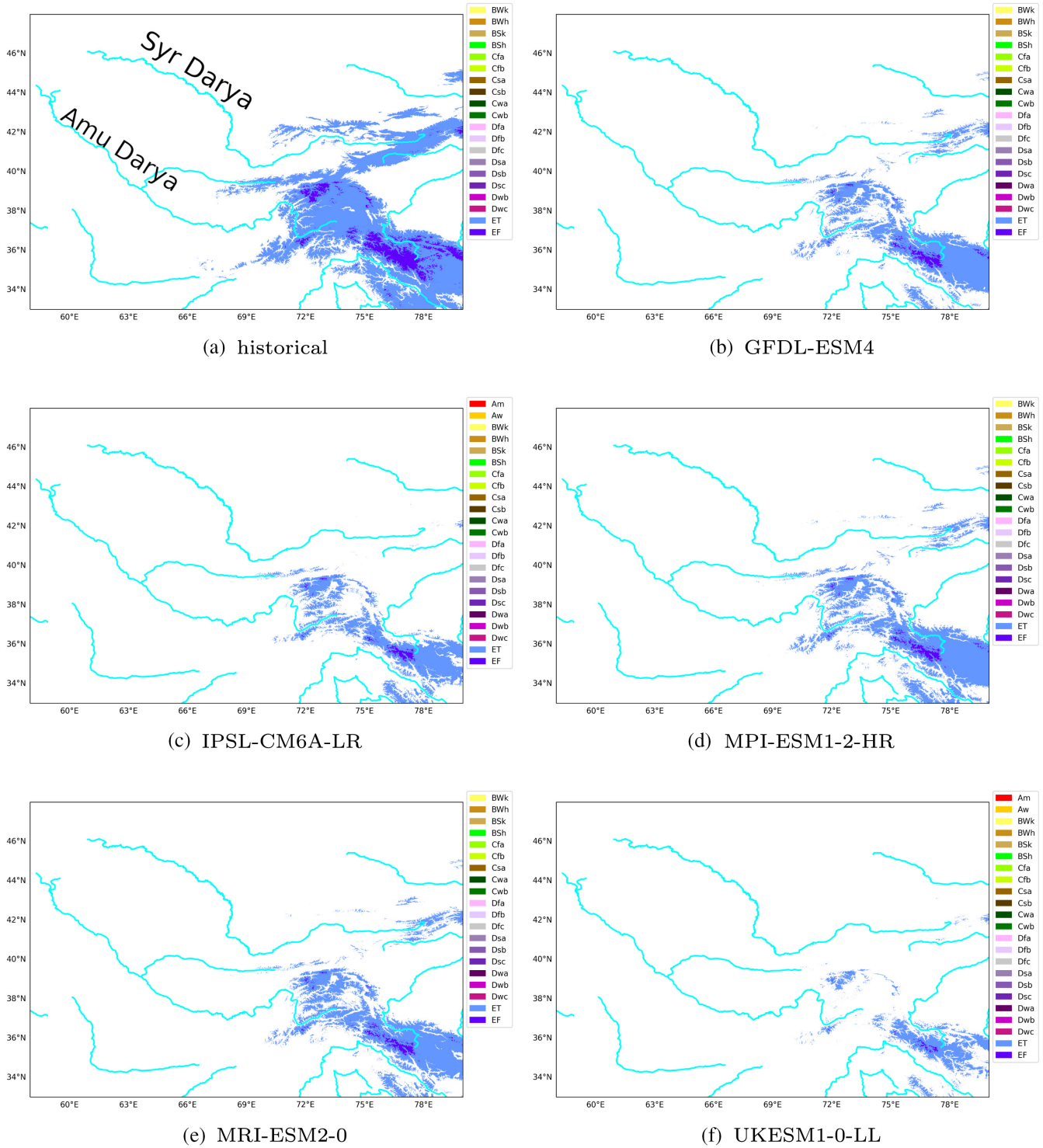

FIGURE 14 Maps of two Köppen climate categories, that is, ET and EF for (a) historical period and at the end of the century (2071–2100) from five model simulations and under ssp585 scenario (b–f) in the two main rivers basins of Central Asia (Amu Darya and Syr Darya).

areas, could lead to decreased albedo and further warming due to lower reflectivity. Reducing cold climate categories could profoundly impact the discharge from the Syr Darya and Amu Darya rivers. Historically, the meltwater from glaciers and snowfields within these climate zones contributes significantly to the flow of these rivers. A decrease in these areas might reduce river flow, especially during the summer when meltwater is a crucial water source. Changes in the hydrological cycle due to reduced snow and ice could affect water availability for agriculture, energy production (hydroelectric), and potable water supply, which are critical for the economies and livelihoods in CA. The anticipated changes call for adaptive strategies to manage water resources more efficiently and explore alternative water supply solutions for the future.

4 | DISCUSSIONS

This study delves into the impacts of climate change across CA, drawing from observed trends and projections provided by CMIP5 and CMIP6 simulations. Our investigation reveals significant warming trends alongside alterations in precipitation, snow depth and runoff—underscoring the acute vulnerability of CA to climate change dynamics. Highlighting extreme climate changes, our analysis brings attention to critical concerns including:

- Expanded arid regions over the last two decades, notably within geopolitically sensitive zones of Afghanistan.
- Notable warming trends during winter months, particularly in CA's mountainous terrains.
- A widespread decline in snow depth and Tundra climate zone across CA.
- Increasingly wetter conditions in regions like East Afghanistan and North Kazakhstan.

Our results corroborate those of Li et al. (2019), who observed similar warming and snow depth reduction trends within the Tian Shan mountains—a critical source of regional water security. Extending beyond these findings, our research elucidates potential temperature and precipitation trends under various future scenarios, predicting a warming range of 2–6°C by the century's conclusion.

The variances between CMIP5 and CMIP6 simulations, particularly CMIP6's higher temperature predictions, highlight the ongoing need for refining climate models. This need aligns with Tapiador et al. (2020), emphasizing the continuous enhancement of climate models to accurately capture the intricate dynamics of regional climates. A noteworthy discovery from our analysis is the consistent linear relationship between precipitation and temperature across observed data and model simulations, suggesting a robust feature that merits further investigation.

The anticipated reduction in snow depth and changes in runoff patterns pose significant concerns for water availability in CA, echoing worries articulated by Barandun et al. (2020), Gan et al. (2015) and White et al. (2014). The progression towards drier conditions, particularly in critical basins such as the Amu Darya and Syr Darya, threatens to exacerbate water scarcity, impacting agriculture, hydropower and potable water supplies.

Moreover, observed and projected shifts in Köppen climate classifications suggest considerable alterations in regional climate regimes, potentially affecting ecosystems, agriculture, and human health. These shifts corroborate findings by Cui et al. (2021), who documented similar transitions towards warmer climate categories in arid regions.

5 | CONCLUSION

Our comprehensive examination of climate change impacts in Central Asia paints a concerning future scenario, marked by significant warming, altered precipitation patterns and ensuing hydrological and ecological challenges. Our findings add to the growing body of evidence advocating for urgent mitigation and adaptation strategies to safeguard water resources, preserve ecosystems and maintain regional stability amidst climate change.

Notably, strategic areas like the Tian Shan mountains—vital "water towers" for CA—are witnessing a significant increase in extreme events, laying bare the potential for added environmental stressors. Projected temperature trends across RCP and SSP scenarios indicate a looming temperature rise of 2–6°C by the century's end, compared to the reference period of 1976–2005, with CA expected to surpass the critical 2 K warming threshold by 2030.

While our analysis spans 70 years of data, capturing a comprehensive spatial detail of potential climate regimes, it is essential to consider the limitations of the observational dataset and the lack of bias-adjustment in climate model simulations. Further, the linear relationship observed between precipitation and temperature, amidst CA's diverse climate drivers, offers a fertile ground for future research endeavours. As we face an increased persistence in critical weather patterns across the Northern Hemisphere, evaluating hydro-climatic risks in CA's vulnerable zones becomes imperative.

The potential reasons behind the warmer and wetter CMIP6 simulations compared to CMIP5, possibly due to enhanced model resolution capturing the complex topography of CA more effectively, warrant further investigation. Importantly, our projections are based on scenarios excluding direct human interventions, like political decisions on water management—highlighted by the Aral Sea's desiccation, primarily due to mismanagement rather than climatic factors alone. This underscores the intricate interplay between human actions and natural changes, emphasizing the need for integrated approaches that combine climate projections with governance strategies to effectively manage water resources.

While the large-scale climatic changes depicted in this study lay the groundwork for understanding climate dynamics in Central Asia, considerable attention and effort must be dedicated to regional climate impact studies. Such targeted research is crucial for devising localized adaptation and mitigation strategies that address this region's unique environmental, societal, and economic challenges.

Cross-disciplinary studies are essential to explore the socio-economic impacts of climate change in CA, especially regarding water resource management and agricultural practices. Initiatives like the Green Central Asia project (https://www.greencentralasia.org/en, last accessed on April 3, 2024) underscore the critical role of international cooperation in developing and implementing adaptation and mitigation strategies, addressing the complex challenges climate change poses to CA.

AUTHOR CONTRIBUTIONS

Bijan Fallah: Conceptualization; software; methodology; validation; visualization; investigation; writing – original draft; writing – review and editing; resources; supervision; data curation; formal analysis. **Iulii Didovets:** Writing – review and editing; visualization; project administration; writing – original draft; methodology. **Masoud Rostami:** Methodology; writing – review and editing; writing – original draft; supervision. **Mehdi Hamidi:** Writing – review and editing; supervision.

ACKNOWLEDGEMENTS

We wish to thank Christoph Menz for providing the model comparison tool for analysis of the CMIP5 and CMIP6 simulations. BF and ID are funded by German Foreign Office via Green Central Asia project (https://www.greencentralasia.org/en). MR is grateful for the support provided by Virgin Unite USA, Inc. through the Planetary Boundary Science Lab project. MH gratefully acknowledges the Alexander von Humboldt Foundation for awarding the George Forster Experienced Researcher Fellowship and its support. Open Access funding enabled and organized by Projekt DEAL.

CONFLICT OF INTEREST STATEMENT

The authors declare no conflicts of interest.

DATA AVAILABILITY STATEMENT

Additional data will be made available at a reasonable request. For the study's open-source data, we refer to the section 2 and Table 1. The Python code for analysing the Köpen classification data is available at GitHub (https://github.com/bijanf/CHELSA_KG_analysis).

ORCID

Bijan Fallah https://orcid.org/0000-0003-3302-2030
Masoud Rostami https://orcid.org/0000-0003-1730-5145

REFERENCES

Adler, R.F., Huffman, G.J., Chang, A., Ferraro, R., Xie, P.P., Janowiak, J. et al. (2003) The version-2 global precipitation climatology project (GPCP) monthly precipitation analysis (1979–present). *Journal of Hydrometeorology*, 4(6), 1147–1167.

Ashraf, S., Nazemi, A. & AghaKouchak, A. (2021) Anthropogenic drought dominates groundwater depletion in Iran. *Scientific Reports*, 11(1), 1–10. Available from: https://doi.org/10.1038/s41598-021-88522-y

Barandun, M., Fiddes, J., Scherler, M., Mathys, T., Saks, T., Petrakov, D. et al. (2020) The state and future of the cryosphere in Central Asia. *Water Security*, 11, 100072.

Chen, Y., Li, W., Deng, H., Fang, G. & Li, Z. (2016) Changes in Central Asia's water tower: past, present and future. *Scientific Reports*, 6, 1–12. Available from: https://doi.org/10.1038/srep35458

Chen, Y., Li, Z., Fan, Y., Wang, H. & Deng, H. (2015) Progress and prospects of climate change impacts on hydrology in the arid region of northwest China. *Environmental Research*, 139, 11–19. Available from: https://doi.org/10.1016/j.envres.2014.12.029

Cucchi, M., Weedon, G.P., Amici, A., Bellouin, N., Lange, S., Schmied, H.M. et al. (2020) WFDE5: bias-adjusted ERA5 reanalysis data for impact studies. *Earth System Science Data*, 12(3), 2097–2120. Available from: https://doi.org/10.5194/essd-12-2097-2020

Cui, D., Liang, S. & Wang, D. (2021) Observed and projected changes in global climate zones based on Köppen climate classification. *Wiley Interdisciplinary Reviews: Climate Change*, 12(3), e701.

Diamond, H.J. & Schreck, C.J. (2020) State of the climate in 2019 the tropics. *Bulletin of the American Meteorological Society*, 101(8), S185–S238. Available from: https://doi.org/10.1175/BAMS-D-20-0077.1

Didovets, I., Lobanova, A., Krysanova, V., Menz, C., Babagalieva, Z., Nur Batsina, A. et al. (2021) Central Asian rivers under climate change: impacts assessment in eight representative catchments. *Journal of Hydrology: Regional Studies*, 34, 100779. Available from: https://doi.org/10.1016/j.ejrh.2021.100779

Dilinuer, T., Yao, J.-Q., Chen, J., Mao, W.-Y., Yang, L.-M., Yeernaer, H. et al. (2021) Regional drying and wetting trends over central asia based on Köppen climate classification in 1961–2015. *Advances in Climate Change Research*, 12(3), 363–372.

Duan, W., Chen, Y., Zou, S. & Nover, D. (2019) Managing the water-climate-food nexus for sustainable development in Turkmenistan. *Journal of Cleaner Production*, 220, 212–224. Available from: https://doi.org/10.1016/j.jclepro.2019.02.040

Gan, R., Luo, Y., Zuo, Q. & Sun, L. (2015) Effects of projected climate change on the glacier and runoff generation in the Naryn River basin, Central Asia. *Journal of Hydrology*, 523, 240–251.

Gao, X., Zhu, Q., Yang, Z., Liu, J., Wang, H., Shao, W. et al. (2018) Temperature dependence of hourly, daily, and event-based precipitation extremes over China. *Scientific Reports*, 8(1), 17564. Available from: https://doi.org/10.1038/s41598-018-35405-4

Geiger, R. & Pohl, W. (1954) Eine neue wandkarte der klimagebiete der erde nach w. Köppens klassifikation (a new wall map of the climatic regions of the world according to w. Köppen's classification). *Erdkunde*, 8, 58–61.

He, H., Luo, G., Cai, P., Hamdi, R., Termonia, P., De Maeyer, P. et al. (2021) Assessment of climate change in Central Asia from 1980 to 2100 using the Köppen geiger climate classification. *Atmosphere*, 12(1), 123.

Hersbach, H., Bell, B., Berrisford, P., Hirahara, S., Horányi, A., Muñoz-Sabater, J. et al. (2020) The ERA5 global reanalysis. *Quarterly Journal of the Royal Meteorological Society*, 146(730), 1999–2049. Available from: https://doi.org/10.1002/qj.3803

Jalilov, S.M., Keskinen, M., Varis, O., Amer, S. & Ward, F.A. (2016) Managing the water-energy-food nexus: gains and losses from new water development in Amu Darya River basin. *Journal of Hydrology*, 539, 648–661. Available from: https://doi.org/10.1016/j.jhydrol.2016.05.071

Karger, D.N., Chauvier, Y. & Zimmermann, N.E. (2023) chelsa-cmip6 1.0: a python package to create high resolution bioclimatic variables based on chelsa ver. 2.1 and cmip6 data. *Ecography*, 2023, e06535.

Karger, D.N., Conrad, O., Böhner, J., Kawohl, T., Kreft, H., Soria-Auza, R.W. et al. (2017) Climatologies at high resolution for the earth's land surface areas. *Scientific Data*, 4(1), 1–20.

Karger, D.N., Wilson, A.M., Mahony, C., Zimmermann, N.E. & Jetz, W. (2021) Global daily 1 km land surface precipitation based on cloud cover-informed downscaling. *Scientific Data*, 8(1), 307.

Kendall, M. (1975) *Rank correlation methods*. Oxford: Oxford University Press.

Kottek, M., Grieser, J., Beck, C., Rudolf, B. & Rubel, F. (2006) World map of the Koppen–Geiger climate classification updated. *Meteorologische Zeitschrift*, 15, 259–263.

Lange, S. (2021) *WFDE5 over land merged with ERA5 over the ocean (W5E5). V.1.0*. GFZ Data Services. Available from: https://doi.org/10.5880/pik.2019.023

Lemenkova, P. (2014) Current problems of water supply and usage in Central Asia, Tian Shan Basin. *Environmental and Climate Technologies*, 3, 11–15. Available from: https://doi.org/10.7250/iscect.2013.002

Li, Y., Tao, H., Su, B., Kundzewicz, Z.W. & Jiang, T. (2019) Impacts of 1.5°C and 2°C global warming on winter snow depth in Central Asia. *Science of the Total Environment*, 651, 2866–2873.

Lioubimtseva, E. & Henebry, G.M. (2009) Climate and environmental change in arid Central Asia: impacts, vulnerability, and adaptations. *Journal of Arid Environments*, 73(11), 963–977. Available from: https://doi.org/10.1016/j.jaridenv.2009.04.022

Lu, G.Y. & Wong, D.W. (2008) An adaptive inverse-distance weighting spatial interpolation technique. *Computers & Geosciences*, 34(9), 1044–1055.

Mann, H.B. (1945) Nonparametric tests against trend. *Econometrica*, 13(3), 245–259. Available from: https://doi.org/10.2307/1907187

Meinshausen, M., Nicholls, Z.R., Lewis, J., Gidden, M.J., Vogel, E., Freund, M. et al. (2020) The shared socio-economic pathway (SSP) greenhouse gas concentrations and their extensions to 2500. *Geoscientific Model Development*, 13(8), 3571–3605. Available from: https://doi.org/10.5194/gmd-13-3571-2020

Palmer, W.C. (1965) Meteorological drought. *US Weather Bureau Research Paper*, 45, 1–58.

Peel, M.C., Finlayson, B.L. & McMahon, T.A. (2007) Updated world map of the Köppen–Geiger climate classification. *Hydrology and Earth System Sciences*, 11(5), 1633–1644.

Pekel, J.F., Cottam, A., Gorelick, N. & Belward, A.S. (2016) High-resolution mapping of global surface water and its long-term changes. *Nature*, 540(7633), 418–422. Available from: https://doi.org/10.1038/nature20584

Peterson, T.C., Folland, C.C., Gruza, G., Hogg, W., Mokssit, A. & Plummer, N. (2001) *Report on the activities of the working group on climate change detection and related rapporteurs 1998–2001*. Geneva: WMO. WCDMP-47, WMO-TD 1071, p. 143. Available from: http://etccdi.pacificclimate.org/docs/wgccd.2001.pdf

Reyer, C.P., Otto, I.M., Adams, S., Albrecht, T., Baarsch, F., Cartsburg, M. et al. (2017) Climate change impacts in Central Asia and their implications for development. *Regional Environmental Change*, 17(6), 1639–1650. Available from: https://doi.org/10.1007/s10113-015-0893-z

Robinson, A., Lehmann, J., Barriopedro, D., Rahmstorf, S. & Coumou, D. (2021) Increasing heat and rainfall extremes now far outside the historical climate. *npj Climate and Atmospheric Science*, 4(1), 45. Available from: https://doi.org/10.1038/s41612-021-00202-w

Santer, B., Po-Chedley, S., Zelinka, M., Cvijanovic, I., Bonfils, C., Durack, P. et al. (2018) Human influence on the seasonal cycle of tropospheric temperature. *Science*, 361, eaas8806. Available from: https://doi.org/10.1126/science.aas8806

Saponaro, A., Pilz, M., Wieland, M., Bindi, D., Moldobekov, B. & Parolai, S. (2015) Landslide susceptibility analysis in data-scarce regions: the case of Kyrgyzstan. *Bulletin of Engineering Geology and the Environment*, 74(4), 1117–1136. Available from: https://doi.org/10.1007/s10064-014-0709-2

Stouffer, R.J. & Wetherald, R.T. (2007) Changes of variability in response to increasing greenhouse gases. Part I: temperature. *Journal of Climate*, 20(21), 5455–5467. Available from: https://doi.org/10.1175/2007JCLI1384.1

Tapiador, F.J., Navarro, A., Moreno, R., Sánchez, J.L. & García-Ortega, E. (2020) Regional climate models: 30 years of dynamical downscaling. *Atmospheric Research*, 235, 104785.

Van Der Schrier, G., Barichivich, J., Briffa, K.R. & Jones, P.D. (2013) A scPDSI-based global data set of dry and wet spells for 1901-2009. *Journal of Geophysical Research: Atmospheres*,

118(10), 4025–4048. Available from: https://doi.org/10.1002/jgrd.50355

van der Wiel, K. & Bintanja, R. (2021) Contribution of climatic changes in mean and variability to monthly temperature and precipitation extremes. *Communications Earth and Environment*, 2(1), 1. Available from: https://doi.org/10.1038/s43247-020-00077-4

van Vuuren, D.P., Edmonds, J., Kainuma, M., Riahi, K., Thomson, A., Hibbard, K. et al. (2011) The representative concentration pathways: an overview. *Climatic Change*, 109(1), 5–31. Available from: https://doi.org/10.1007/s10584-011-0148-z

Vörösmarty, C.J., McIntyre, P.B., Gessner, M.O., Dudgeon, D., Prusevich, A., Green, P. et al. (2010) Global threats to human water security and river biodiversity. *Nature*, 467(7315), 555–561. Available from: https://doi.org/10.1038/nature09440

Weedon, G.P., Balsamo, G., Bellouin, N., Gomes, S., Best, M.J. & Viterbo, P. (2014) Data methodology applied to ERA-Interim reanalysis data. *Water Resources Research*, 50, 7505–7514. Available from: https://doi.org/10.1002/2014WR015638. Received

White, C.J., Tanton, T.W. & Rycroft, D.W. (2014) The impact of climate change on the water resources of the amu darya basin in central asia. *Water Resources Management*, 28, 5267–5281.

Yang, P., Zhang, Y., Xia, J. & Sun, S. (2020) Identification of drought events in the major basins of Central Asia based on a combined climatological deviation index from GRACE measurements. *Atmospheric Research*, 244, 105105. Available from: https://doi.org/10.1016/j.atmosres.2020.105105

Yao, J., Chen, Y., Chen, J., Zhao, Y., Tuoliewubieke, D., Li, J. et al. (2021) Intensification of extreme precipitation in arid Central Asia. *Journal of Hydrology*, 598, 125760. Available from: https://doi.org/10.1016/j.jhydrol.2020.125760

SUPPORTING INFORMATION

Additional supporting information can be found online in the Supporting Information section at the end of this article.

How to cite this article: Fallah, B., Didovets, I., Rostami, M., & Hamidi, M. (2024). Climate change impacts on Central Asia: Trends, extremes and future projections. *International Journal of Climatology*, *44*(10), 3191–3213. https://doi.org/10.1002/joc.8519